buildings

MDPI

Article

Physico-Antibacterial Feature and SEM Morphology of Bio-Hydraulic Lime Mortars Incorporating Nano-Graphene Oxide and Binary Combination of Nano-Graphene Oxide with Nano Silver, Fly Ash, Zinc, and Titanium Powders

Mehmet Serkan Kırgız [1,*], Jahangir Mirza [2,*], Stanca Cuc [3,*], Doina Prodan [3,*], Codruţa Saroşi [3], Ioana Perhaiţă [3], Rahela Carpa [4], Marioara Moldovan [3], Dorin Popa [5], Simona Varvara [5] and Maria Popa [6]

1 Northwestern University, Chicago, IL 60208-001, USA
2 Faculty of Civil and Environmental Engineering, York University, Toronto, ON M3J 1P3, Canada
3 "Raluca Ripan" Chemistry Research Institute, Babeş Bolyai University, 400084 Cluj-Napoca, Romania
4 Department of Molecular Biology and Bio-Technology, Faculty of Biology and Geology, Babes Bolyai University, 400084 Cluj-Napoca, Romania
5 Faculty of Exact Sciences and Engineering, 1 Decembrie 1918 University of Alba Iulia, 510009 Alba Iulia, Romania
6 Faculty of Economic Sciences, 1 Decembrie 1918 University of Alba Iulia, 510009 Alba Iulia, Romania
* Correspondence: nakres42@yahoo.com (M.S.K.); mirza7861@gmail.com (J.M.); stanca.boboia@ubbcluj.ro (S.C.); doina.prodan@ubbcluj.ro (D.P.)

Abstract: The study evaluated the impact of graphene powders used as additives in the recipe of the experimental lime mortar to a mixture ratio of 1:2.5 of NHL3.5 hydraulic lime:fine sand. The content of binder, aggregate and water was kept constant, varying only the amount and the type of the added additives in relation to the amount of natural hydraulic lime NHL3.5. The following five types of experimental mortars were prepared as follows: reference mortar (without additive); mortars containing 1 wt.% GO and 5 wt.% GO powder; mortar with the following GO powders mixture: GO powder functionalized with silver nanoparticles and with fly ash (GO-Ag + GO-fly ash); mortar with the following GO powders mixture: GO with zinc oxide and with titanium oxide (GO-ZnO + GO-TiO_2). The influence of the GO-based additive addition on the porosity, surface microstructure, and water sorption coefficient of the mortar samples was evaluated. The antibacterial effect of the mortar samples against three bacterial strains was also investigated. The best results were obtained for the experimental mortar containing GO-ZnO -TiO_2, which showed improved experimental properties that potentially allow its use for the rehabilitation of heritage buildings.

Keywords: graphene nanopowder; hydraulic mortar; porosity; water absorption; antibacterial property; SEM morphology

check for updates

Citation: Kırgız, M.S.; Mirza, J.; Cuc, S.; Prodan, D.; Saroşi, C.; Perhaiţă, I.; Carpa, R.; Moldovan, M.; Popa, D.; Varvara, S.; et al. Physico-Antibacterial Feature and SEM Morphology of Bio-Hydraulic Lime Mortars Incorporating Nano-Graphene Oxide and Binary Combination of Nano-Graphene Oxide with Nano Silver, Fly Ash, Zinc, and Titanium Powders. *Buildings* **2023**, *13*, 172. https://doi.org/10.3390/buildings13010172

Academic Editors: Christopher Yu-Hang Chao and Antonin Fabbri

Received: 16 October 2022
Revised: 7 December 2022
Accepted: 6 January 2023
Published: 9 January 2023

Copyright: © 2023 by the authors. Licensee MDPI, Basel, Switzerland. This article is an open access article distributed under the terms and conditions of the Creative Commons Attribution (CC BY) license (https://creativecommons.org/licenses/by/4.0/).

1. Introduction

Natural hydraulic lime [1] represents a binder class, which is especially compatible with the binders used in the rehabilitation and preservation of the masonry of heritage buildings [2,3].

The literature already contains many reports about the characteristics of the mortar formulated with NHL 3.5 natural hydraulic lime, which meets the requirements of the EN 459-1 standard [1,4]. Most of the reported recipes had a volumetric ratio of 1:3 (lime:sand), from which various percentages of the mass of lime were replaced with different fillers, such as a fine fraction of ceramics from the facade tile [5] or bricks and pots [6,7]. The incorporation of these fillers induced various changes in the characteristics and properties of the hardened mortar [8,9]. The major characteristic that lime mortars must meet for a correct validation is a good preservation of the material over time.

The environmental factors, along with the composition and the specific properties of the used materials might determine various degradation processes [10]. Among the factors that influence the degradation of the material over time are their composition (type and amount of binder, particle size distribution of sand) and properties (porosity, capillary transport, and adhesion to the substrate). Other important degradation factors of lime mortars are mainly the humidity and weather conditions. The behavior of the water is particularly relevant for the overall performance of the plasters applied to the old masonry. In fact, plasters and mortars must protect the masonry against water, preventing the easy infiltration of high volumes of water, and promoting their rapid drying [11]. In addition to the presence of water and meteorological phenomena, buildings can be colonized by various microorganisms (microalgae, fungi, lichens, and moss) that can spread to the surface of interior building materials under certain conditions of temperature, humidity (water flow and/or high relative humidity), and sunlight [12,13].

In recent years, graphene [14,15] was included in the composition of mortars being effective in controlling the durability and mechanical properties of building materials [16,17]. The interest in incorporating graphene as an additive into cement-based materials is determined by the potential multifunctionality it can give to concrete and mortar [18]. There are reports in the literature indicating that very small additions (from 0.04 to 0.08 wt.%) of GO powder into the cement composition could lead to an improvement in mechanical strength [19,20]. In their study, Faria et al. [14] investigated the influence of GO powder on the microstructure and mechanical and physical properties of hydraulic lime-based mortars that could be intended for building rehabilitation. The addition of 0.05 wt.% and 0.1 wt.% of GO led to slightly improved mechanical properties, while the sample containing 0.1 wt.% GO presented a better durability under the action of water [14].

Wang et al. [21] proved that the antibacterial effect of the ZnO/GO combination depends on the content of zinc, and this composite material can be potentially used as a disinfection agent in the surface coating on various substrates. There is a synergistic effect between ZnO and GO that provides an increase in the contact of bacteria with zinc due to the release of ions from the zinc nanoparticles that cover the graphene sheets and surround the bacteria, ultimately leading to their inactivation [21].

It is known from the authors of [22,23] that the addition of between 0.01 and 10 ppmv (parts per million volume) of TiO_2 in the mortars allows the improvement of the indoor air quality in buildings where the ventilation systems or air purifiers are not efficient, contributing to the reduction of the air pollutants concentration. It was also reported that TiO_2-incorporating mortars can be applied in historic buildings because the TiO_2 nanoadditive does not compromise the properties of the hardened mortar [22], thus offering an effective solution for cleaning the air inside the old buildings. Nowadays, a commercial cement with photocatalytic properties (TioCem) could be found on the market and used for covering the walls of buildings in order to purify the air inside. Apart from the mortar, TiO_2 nanoparticles have been also incorporated into other materials, such as plaster, concrete, etc. [24]. Following the photocatalytic reaction, the gaseous pollutants from the air are adsorbed on the surface of these composite materials. After their removal, the TiO_2-incorporating material is active again, being able to lead to a new photocatalytic process [25].

Noeiaghaei et al. [26] explored the bactericidal characteristics of the cementitious materials surface treated with ZnO and Ag nanoparticles. They monitored the development of the gram-positive *Bacillus cereus* and the gram-negative *Escherichia coli* bacterial strains at different pH levels on the surface of the mortar samples. It was found that at a concentration of 250 mg/l of nanoparticles, after seven days, the cell viability decreased by more than 60% in both cases and at all tested pH values. The gram-positive strain appears to be less sensitive than the gram-negative strain to both ZnO and Ag nanoparticles.

The possibility to replace a part of the cement mortars with fly ash was investigated by Ibrahim et al. [27]. Various percentages of cement, namely, 0%, 5%, 10%, 15%, and 20% were replaced with fly ash, and different tests were carried out, such as compressive strength,

water absorption, etc. It was found that the mortar containing 15% fly ash has the highest compressive strength after 28 days. Moreover, all the investigated mortars containing fly ash present good physical–mechanical properties. It was also reported that the addition of GO powder with fly ash can improve the resistance of the material to the sulfate attack and also contributes to better mechanical resistance. GO can lead to the formation of nucleation centers in the binder pores, leading to an increase in hydration products [9,28,29].

Based on previous studies [30], in the present paper, new mortar samples containing various ratios of different additives, namely, GO powder or mixtures of various functionalized GO powder were prepared. The influence of the additive's nature and ratio in the mixtures on the mortar's porosity, water absorption coefficient, antibacterial effect, and surface structure was closely examined and compared with the characteristic of the classic hydraulic lime mortar.

2. Materials and Methods

2.1. Materials

The mortars used in this research contain lime, sand, water, and various additives such as the following: graphene oxide powder, or mixtures of functionalized graphene oxide powder, meant to improve the characteristics of the classic hydraulic lime mortar. The experimental additives into the composition of the mortars were obtained in UBB-ICCRR (Cluj-Napoca-Romania) [31]. The binder used was a natural hydraulic lime NHL3.5 produced by La Banca della Calce (Bologna, Italy), according to UNI EN 459-1: 2010, CE marked [1] By introducing the binder into the composition, the mortars are easy to apply both manually and mechanically, with a slow curing process, that makes the mortar ductile and workable for a long time, making it the most suitable binder in ecological constructions (Bio-Constructions) [32].

The binder/aggregate ratio was 1:2.5. A fine sand was used, with the particle size distribution from a few tens of microns to 1 mm. The water/mixture (binder and additive) ratio was 1.05. The content of binder, aggregate, and water was kept constant, varying only the amount and type of additive in relation to the amount of natural hydraulic lime NHL3.5.

Five types of hydraulic lime mortars were prepared as follows: reference mortar (M), without any additive; mortar containing 1 wt.% GO (M1); mortar with 5 wt.% GO powder (M2); mortar with 5 wt.% additive mixtures based on powders with GO functionalized with silver nanoparticles, respectively GO functionalized with fly ash (GO-Ag + GO-fly ash) (M3) and mortar with 5 wt.% additive mixtures based on powders with GO functionalized with zinc oxide, respectively GO functionalized with titanium oxide (GO-ZnO + GO-TiO_2) (M4).

The synthesis of graphene oxide powder (GO) used as additive in this study was achieved by the Hummer method [33]. A part of the GO powder was functionalized with Ag, in a mass ratio of 2:1. The other parts of GO powder were functionalized with ZnO, TiO_2, and, respectively, with fly ash, in a ratio of 1:20. The powders with functionalized graphene were then silanized with the silane ATPS (3-aminopropyl) triethoxysilane silane) and were characterized in a previous study [31]. The silanization of the powders with GO was carried out with the aim of increasing the adhesion of the mortar by introducing them as additives in its composition. The previous functionalization of the graphene powders was made aiming to obtain a potential antibacterial effect that would be very beneficial in the restoration of heritage buildings, especially in areas contaminated with fungi and bacteria. In our previously reported study, the influence of the silanization process on the antibacterial effect of the GO powders was also demonstrated and the obtained results were promising [31]. Identification of the mortar mixtures and their composition are shown in Table 1.

Table 1. The quantity of lime, sand, water, and GO-based powders as kg for m^3 in the control sample and experimental mortars.

Mortar Code	Lime/Sand [*v*/*v*]	Lime [kg]	Sand [kg]	Water [L]	GO Type		GO [kg]	
M	1/2.5	452.26	1941.7	474.87	0		0	
M1	1/2.5	452.26	1941.7	474.87	GO		4.52	
M2	1/2.5	452.26	1941.7	474.87	GO		22.6	
M3	1/2.5	452.26	1941.7	474.87	GO-Ag	GO-fly ash	11.3	11.3
M4	1/2.5	452.26	1941.7	474.87	GO-ZnO	GO-TiO_2	11.3	11.3

2.2. Sample Preparation and Strengthening

Five hydraulic mortar samples containing various concentrations of different experimental additives based on graphene oxide/mixture of functionalized graphene were obtained (GO, GO-Ag-fly ash, GO-ZnO-TiO_2). The experimental additives were previously weighed in the laboratory, just like the binder. An efficient mixing of the two components was performed beforehand (15 min). The preparation of the mortar paste was performed in the same way as in the case of any mortar, following the recipe and adding water gradually.

The molds containing the mortar samples were initially covered with a polyethylene film for initial hardening. During the next day, the film was removed, and an attempt was made to separate the edges of the samples. The samples were further left in the molds for the next 24 h. The curing of the samples was achieved in the laboratory, at a temperature of 20 ± 2 °C. All tests were carried out after 28 days.

2.3. Characterization Techniques

2.3.1. Analysis of Specific Surface and Porosity

The specific surface and porosity of the powders were determined using the technique of physical adsorption of inert gas on the surface and in the pores of the material, using the "Tri Star II 3020" Analyzer—Micromeritics. Before the porosity measurements, the samples were treated by decontamination/degassing at 50 °C, for 24 h, in a nitrogen stream. Nitrogen adsorption–desorption isotherms are measured at a temperature close to their boiling point (77 K; −321°F). The pressure of the adsorbent gas gradually increases, up to the saturation value, when the condensation of the adsorbate (N_2) takes place in the pores. As the pressure rises, the amount of gas adsorbed on the surface and pores of the solid material will increases, too.

2.3.2. Determination of Water Absorption Coefficient

The determination of the water absorption coefficient due to the capillary action of the hardened mortar was performed according to EN 1015-18: 2002 and UNI EN 15801: 2010 [34,35].

The specimens were obtained in prismatic silicone molds of 40 × 40 × 160 mm, and after 28 days of hardening they were dried to constant mass in a ventilated oven at 60 °C ± 5 °C, obtaining M0—dry mass of the specimen (g). After the side edges of the prism were sealed with epoxy resin, the specimens were immersed in water up to 2 mm height. The determinations were performed at the following different intervals: 5, 10, 30, 60, 90 min, and 1440 min (24 h), respectively. After each immersion, the specimens were weighed to obtain the Mi—mass of the specimen after contact with water at a certain time (minutes). The amount of water absorbed by the specimens per unit area at time t ~ (s) was calculated according to the following formula: Q = [(Mi − M0)/A], [kg/m^2], where A is the area of water contact surface [m^2].

2.3.3. The Antibacterial Effect of Hardened Mortars after 28 Days

To investigate the antibacterial effects, the mortar samples (5 mm in diameter × 2 mm high) were hardened and stored for 28 days in plastic molds.

The equal amounts of investigated samples were placed in 5 mm wells of the Petri dishes and inoculated with three bacterial strains, then incubated for 24 h at 37 °C.

The microorganisms tested in this study were as follows: *Enterococcus faecalis* ATCC 29212, *Escherichia coli* ATCC 25922, *Staphylococcus aureus* ATCC 25923, from the collection of the Laboratory of Microbiology, Faculty of Biology and Geology, UBB, Cluj.

Each bacterial strain was grown for 24 h on Nutrient Agar medium. A dilution of 0.5 McFarland in sterile saline was made from each strain. From these dilutions, each Petri dish is inoculated with a sterile swab soaked in 0.5 McFarland microbial suspension and spread over the entire surface of the solid culture medium.

2.3.4. Morphological and Structural Characterization by Scanning Electron Microscopy (SEM)

The morphological and structural characterization of the mortar surfaces was performed using an Inspect S electron microscope (FEI Hillsboro, OR, USA) at low vacuum, with an acceleration voltage of 30 kV and magnifications ×100. The SEM analysis was performed in low vacuum on the detached mortar pieces, following the mechanical tests, after 28 days, without applying any other treatment to the samples.

3. Results

3.1. Analysis of Specific Surface and Porosity

The isotherms of the samples are similar to type IV, according to the IUPAC classification, characteristic of mesoporous adsorbents, with pores in the range of 2–50 nm. The hysteresis formed by the adsorption–desorption isotherms is of H3 type, suggesting the presence of crack-type pores in the powders.

According to Figure 1 and Table 2, the amount of nitrogen adsorbed in the pores of the samples decreases with the addition of various additives in the mortar, from 8.7 cm^3/g STP (M) to 5.1 cm^3/g STP (M3), 3.3 cm^3/g STP (M2) and 2.8 cm^3/g STP (M4), respectively, which reduces the specific sample area substantially from 1.822 m^2/g (M) to 1.137 m^2/g (M3), 0.626 m^2/g (M2) and 0.275 m^2/g (M4).

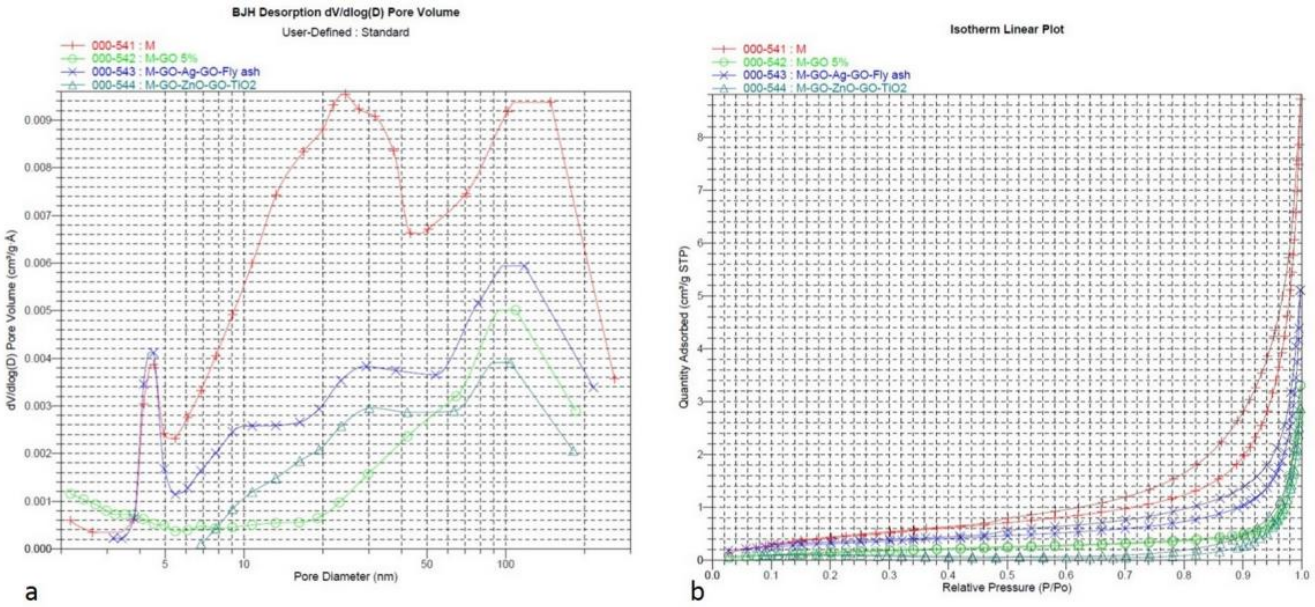


Figure 1. (**a**) Distribution and pore volume in mortars M, M2, M3 and M4 and (**b**) adsorption–desorption isotherms after 28 days.

Table 2. The main surface and porosity characteristics of the analyzed material.

Sample	Sample Weight [g]	Specific Surface Area (BET) [m^2/g]	Volume Mesopores and Macropores 2–300 nm (BJH Desorption) [cm^3/g]	Diameter Medium, Meso and Macropores 2–300 nm (BJH Desorption) [nm]
M	0.3901	1.822	0.0142	23.02
M2	0.4326	0.626	0.0053	27.24
M3	0.4732	1.137	0.0079	24.54
M4	0.4848	0.275	0.0047	40.17

BET—Brunauer, Emmett, Teller method for surface area in the range 0.05–0.3 p/po; BJH—Barett, Joyner, Halenda method for meso size (2–50 nm) and macropores (>50 nm).

The pore volume distribution curves according to their diameter, shown in Figure 1, have a multimodal appearance, which shows dimensional or smaller pores in terms of dimensional pores. For mortar samples M and M3, the pore volume distribution curves show three maximums at 4 nm, 25 nm (mesopores), and 120 nm (macropores). The difference between them is the change in the ratio of the maxima from 25 nm to 120 nm. The pore volume of the M mortar sample (0.014 cm^3/g) is double that of the M3 sample (0.007 cm^3/g), the pores being deeper, but with an average diameter of less than 23.02 nm compared to 24.54 nm (Table 2).

In the case of M2 and M4 mortar samples, the pore volume distribution cubes are bimodal but have a different appearance. M2 mortar, in addition to the macropores highlighted by the maximum from 100 nm, also has a low content of micropores (max. 2 nm), derived from the addition of graphene, so that the average pore diameter is 27.24 nm, when the M4 sample contains, in addition to macropores (max. 100 nm), a consistent volume of mesopores (max. 30 nm), which causes the average pore diameter to increase to 40.17 nm.

3.2. Determination of Water Absorption Coefficient

Table 3 shows the average values of the absorption coefficient of each material at the time (t). Figure 2 shows the average distribution of the amount of water absorbed by each material per unit area Q (kg/m^2) at time $\sqrt{t}$ ~ (s). From Figure 2 and Table 3, it can be seen that the highest values of the absorption coefficient were recorded in the case of control M, followed by M3 at 24 h. The lowest values of the absorption coefficient were recorded for M4.

Table 3. The average value of the initial weight of the samples, the area of contact with water, and the average values of the absorption coefficients.

Sample	M0 [g]	A [mm^2]	Q5 [kg/m^2]	Q10 [kg/m^2]	Q30 [kg/m^2]	Q60 [kg/m^2]	Q90 [kg/m^2]	Q1440 [kg/m^2]
M	250	1600	4.8125	7.84375	13.15625	15.05	18.125	18.7875
M1	232	1600	0.5125	1.6125	3.5875	6.90625	7.5625	9.425
M2	228	1600	0.5625	1.175	2.9375	8.23125	10.93125	15.58125
M3	236	1600	0.0875	0.4	2.2625	6.1625	9.0375	18.0875
M4	249	1600	0.075	0.15625	0.28125	0.475	0.5875	0.90625

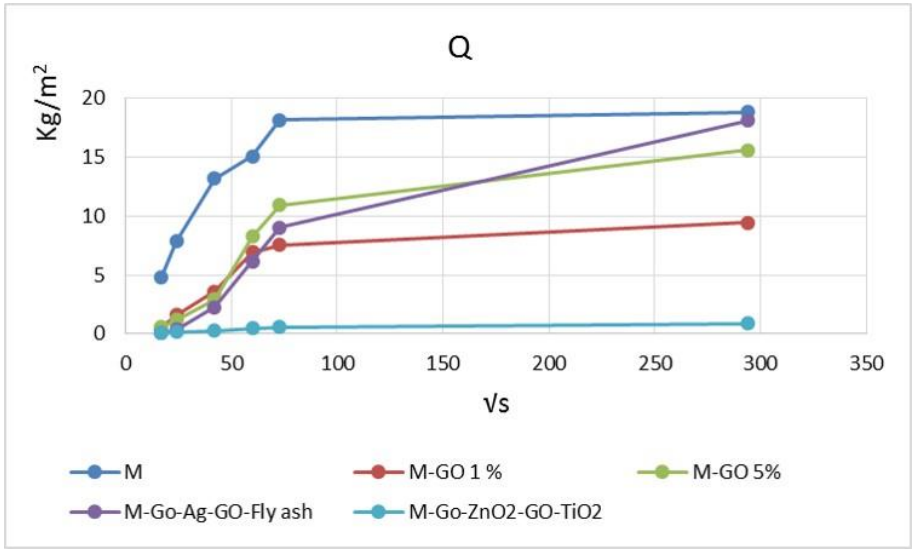


Figure 2. The average water sorption coefficient of the mortars investigated at time (t).

3.3. The Antibacterial Effect of Hardened Mortars after 28 Days

Figure 3 and Table 4 show the average diameters of the bacterial inhibition zone for all tested mortars. The composition of the mortar samples is presented in Table 1. The mortar samples were recorded from M0 to M4 in Figure 3 and Table 4.

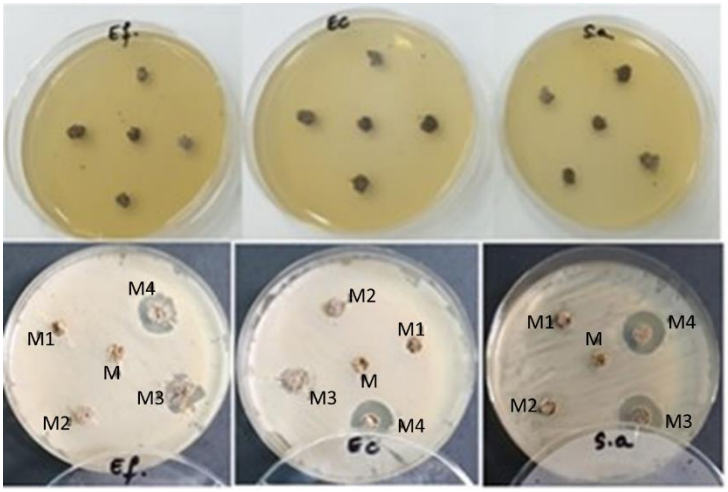


Figure 3. Application of the bacterial strains (*Ef. Ec. Sa.*) on the five tested mortar samples at the time 0 (initially) and after 24 h.

Table 4. Diameter of inhibition zones (mm) of the tested mortar samples.

Sample code/Bacterial Strain	M	M1	M2	M3	M4
Enterococcus faecalis (*Ef.*)	0	0	0	13.5	15
Escherichia coli (*Ec*)	0	0	0	12	16
Staphylococcus aureus (*S.a*)	0	0	0	16	16

As illustrated in Figure 3 and Table 4, the mortar samples show different antimicrobial activity depending on their composition (added additives) and the tested bacterial strain. Although in our previous study [31], the antibacterial effect on the GO samples against the three bacterial strains also used in these tests was clearly demonstrated, in the present investigation, the mortar samples containing 1 wt.% GO (M1) and 5 wt.% GO (M2), as

well as the control sample (M), did not show any antibacterial effect against *Enterococcus faecalis*, *Escherichia coli*, and *Staphylococcus aureus*. Instead, an important bacterial inhibition was noticed in the case of the mortars containing additives based on functionalized GO mixtures, which proves that the compounds added by the functionalization of GO powders acted on the tested bacteria.

3.4. SEM Images of Hardened Mortars

Figure 4 presents the morphological features of different mortar samples obtained by SEM analysis. The microstructure of the reference mortar (Figure 4a) appears as homogeneous and dense, with high porosity and with a carbonate matrix in which two types of crystalline growth occur, i.e., with large and small particles. The images from Figure 4b–d show a good internal cohesion between the mortar components. Considering that the difference between the samples consists only of the added minority components (graphene), it could be inferred that the adhesion between the matrix and the aggregate is influenced by the texture of the aggregate granules and the combinations of added graphene, the texture and nature of these nanoparticles, along with the viscosity of the paste and the surface tension.

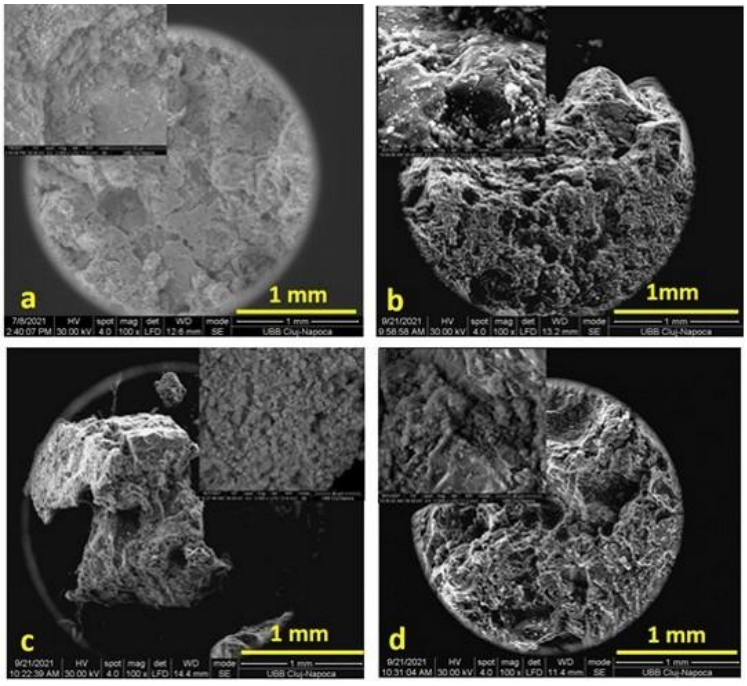


Figure 4. SEM images of M (**a**), M-GO 5% (**b**), M-GO-Ag-fly ash (**c**), and M-GO-ZnO-TiO_2 (**d**) at ×100 revealed a homogenous surface with differences in the texture.

4. Discussion

The main reason for the damage to the construction materials is the presence of water moving through the walls. Mortar porosity is an important factor affecting the movement and evaporation of water and therefore is a key parameter for assessing the durability of a restoration mortar [36]. From Table 2, it was observed that the pore volume of the mortar powders with graphene decreased when compared to the pore volume of the control mortar powder (without graphene). This is due to the migration of nanoparticles inside the mortar pores. The pore volume decreased the most in the mortar added with mixtures of graphenes functionalized with ZnO and TiO_2 when compared to the mortar containing mixtures of graphenes functionalized with Ag and fly ash. A possible explanation could be related to the fact that the ratio GO:Ag is 2:1 in the graphene functionalized with Ag, while in the case of the other GO powders, the ratio between the GO and the metallic oxides or fly ash is 1:20. Therefore, it can be supposed that the shape of the nanoparticles is responsible

for the different porosity of the mortar samples. The two oxides and fly ash have round particles, while the graphenes, having a layered structure with sharp edges, can penetrate more difficult inside the mortar's pores.

In terms of water absorption, it could be noticed that the addition of 5% nanopowder of GO Ag—fly ash and GO TiO_2 -ZnO leads to a decrease in the water absorption. Instead, by the addition of the simple GO nanopowder in the concentration of 5 wt.%, the water absorption increases, reaching the value of the reference mortar, while a lower water absorption capacity value was obtained when 1 wt.% GO powder was added to the mortar sample. The decreased water absorption capacity is a positive factor in reducing the risk of moisture in the walls.

Mohammed et al. [37] also reported that mortars with 0.03 wt.% GO presents a decrease in the water absorption capacity when compared to the reference mortar, due to the smaller pores amount induced by the addition of the GO powder, which therefore reduces the capillary porosity. It was suggested that the addition of GO to the cement composites can improve their resistance to the aggressive elements by interconnecting the GO structure with the cement matrix, which creates a strong barrier and reduces the penetration of aggressive agents.

Recent studies showed that the physical and chemical properties of graphene-based nanomaterials, such as surface functionality [38], morphology [39], concentration, and sheets sizes [40], play a vital role in obtaining and inducing an antimicrobial effect. In our study, the antibacterial effect of the experimental lime mortars containing additives based on the functionalized GO powders mixtures with ZnO—TiO_2 or Ag-fly ash is primarily supported by the presence of GO-ZnO and, respectively, GO-Ag powders, in agreement with other previously reported studies [41–46].

5. Conclusions

In the present paper, natural hydraulic lime mortars incorporating GO sheets functionalized with different nanomaterials were produced and the microstructures of the hardened mortars were investigated regarding their specific surface and porosity, water absorption coefficient, and antibacterial effect.

The mortar samples containing 1 wt.% and 5 wt.% non-functionalized GO powders present slightly improved structures and absorption characteristics, as compared to the conventional mortar, due to the incorporation of GO sheets into the mortar structure. However, the antibacterial tests of 1 wt.% and 5 wt.% non-functionalized GO sheet mortars showed no antimicrobial effects.

Instead, the addition of GO powders functionalized with oxides (TiO_2 and ZnO) or with fly ash and Ag leads to mortars with lower water absorption capacity and significant antibacterial effects on three bacterial strains (*Enterococcus faecalis*, *Escherichia coli*, and *Staphylococcus aureus*). An important decrease in the porosity was also observed in the mortar containing GO powders functionalized with ZnO and TiO_2.

This study provides a good indication that the formulation of NHL3.5 mortars can be optimized in terms of absorption and antibacterial effect by adding in their composition of different mixtures of GO functionalized, as additives. The best performances were noticed for the experimental mortar containing GO powders mixture (with ZnO and TiO_2), followed by mortar with GO powders mixture (with fly ash and Ag).

In the future, it is worth performing some wider microstructural examinations to confirm that the size and shape of the nanoparticles and graphene nanosheets are the only reasons for the porosity changes.

Author Contributions: Conceptualization and resource D.P. (Doina Prodan) and D.P. (Dorin Popa); methodology and data curation M.P.; validation and software M.M. and S.V.; software, conceptualization, data curation, resource I.P., R.C. and S.C.; writing-original draft preparation, C.S.; supervision, writing-review and editing, fund acquisition, software M.S.K. and J.M. All authors have read and agreed to the published version of the manuscript.

Funding: This work was supported by a grant from the Romanian Ministry of Education and Research, CCCDI—UEFISCDI, project number PN-III-P2-2.1-PED-2019-3739, no. 565 PED/2020; by a grant of the Ministry of Research, Innovation and Digitization, CNCS/CCCDI-UEFISCDI, project number COFUND-M-ERANET-3-GEOSUMAT, no. 314/2022.

Data Availability Statement: The data presented in this study are available on request from the corresponding authors. The data are not publicly available due to restrictions applied for corresponding authors' universities.

Conflicts of Interest: The authors declare that the research was conducted in the absence of any commercial or financial relationships that could be construed as a potential conflict of interest.

References

1. *SR EN 459-1: 2010*; Building Lime. Part 1: Definitions, Specifications and Conformity Criteria. European Committee for Standardization: Brussels, Belgium, 2010.
2. Grilo, J.; Santos-Silva, A.; Faria, P.; Gameiro, A.; Veiga, R.; Velosa, A. Mechanical and mineralogical properties of natural hydraulic lime-metakaolin mortars in different curing conditions. *Constr. Build. Mater.* **2014**, *51*, 287–294. [CrossRef]
3. Grilo, J.; Faria, P.; Veiga, R.; Santos-Silva, A.; Silva, V.; Velosa, A. New Natural Hydraulic Lime mortars—Physical and microstructural properties in different curing conditions. *Constr. Build. Mater.* **2014**, *54*, 378–384. [CrossRef]
4. *SR EN 1015-11: 1999*; Methods of Test for Mortar for Masonry. Part 11: Determination of 445 Flexural and Compressive Strength of Hardened Mortar. European Committee for Standardization: Brussels, Belgium, 1999.
5. Faria, P.; Silva, V.; Madeira, T. Natural hydraulic lime mortars with ceramic residues for masonry. In Proceedings of the 9th International Masonry Conference, Guimarães, Portugal, 7–9 July 2014.
6. Faria, P.; Silva, V. Natural Hydraulic Lime Mortars: Influence of the Aggregates. In *Historic Mortars*; Springer: Cham, Switzerland, 2013.
7. Matias, G.; Faria, P.; Torres, I. Viability of Ceramic Residues in Lime-Based Mortars. In *Historic Mortars*; Springer: Cham, Switzerland, 2019; pp. 213–225.
8. Kırgız, M.S. Effects of the colloid graphite Nano-Particle on the properties of fuel ash-green cement composite. *Res. J. Recent Sci.* **2020**, *9*, 19–27, ISSN 2277-2502. [CrossRef]
9. Kirgiz, M.S. Advancements in Properties of Cement Containing Pulverised Fly Ash and Nanomaterials by Blending and Ultrasonication Method (Review-Part I). *Nano Hybrids Compos.* **2018**, *19*, 37–44. [CrossRef]
10. van Hees, R.P.J.; Binda, L.; Papayianni, I.; Toumbakari, E. Characterisation and damage analysis of old mortars. *Mater. Struct.* **2004**, *37*, 644–648. [CrossRef]
11. Rosário Veiga, M.D.; Aguiar, J.; Santos, S.A.; Carvalho, F. Methodologies for characterisation and repair of mortars of ancient buildings Historical Constructions. *Mater. Struct.* **2005**, *38*, 761–769.
12. Heseltine, E.; Rosen, J. (Eds.) *WHO Guidelines for Indoor Air Quality: Dampness and Mould*; World Health Organization: København, Denmark, 2009; ISBN 978-92-890-4168-3.
13. Shirakawa, M.A.; Gaylarde, C.C.; Gaylarde, P.M.; John, V.; Gambale, W. Fungal colonization and succession on newly painted buildings and the effect of biocide. *FEMS Microbiol. Ecol.* **2002**, *39*, 165. [CrossRef]
14. Faria, P.; Duarte, P.; Barbosa, D.; Ferreira, I. New composite of natural hydraulic lime mortar with graphene oxide. *Constr. Build. Mater.* **2017**, *156*, 1150–1157. [CrossRef]
15. Diekamp, A.; Stalder, R.; Konzett, J.; Mirwald, P.W. Lime mortar with natural hydraulic components: Characterisation of reaction rims with FTIR imaging in ATR-mode. *Hist. Mortars* **2012**, *7*, 105–113. [CrossRef]
16. Zhang, C.; Zhu, X.; Wang, Z.; Sun, P.; Ren, Y.; Zhu, J. Facile synthesis and strongly microstructuredependent electrochemical properties of graphene/manganese dioxide composites for supercapacitors. *Nano. Res. Lett.* **2014**, *9*, 490. [CrossRef]
17. Katman, H.B.Y.; Khai, W.J.; Kırgız, M.S.; Nehdi, M.L.; Benjeddou, O.; Thomas, B.S.; Papatzani, S.; Rambhad, K.; Kumbhalkar, M.A.; Karimipour, A. Transforming conventional construction binders and grouts into high-performance nano-carbon-binders and grouts for today's construction. *Buildings* **2022**, *12*, 1041. [CrossRef]
18. Kırgız, M.S. Pulverized fuel ash cement activated by nanographite. *ACI Mater.* **2018**, *115*, 803–812. [CrossRef]
19. Shang, Y.; Zhang, D.; Yang, C.; Liu, Y.; Liu, Y. Effect of graphene oxide on the rheological properties of cement pastes. *Constr. Build. Mater.* **2015**, *96*, 20–28. [CrossRef]
20. Pan, Z.; He, L.; Qiu, L.; Korayem, A.H.; Li, G.; Zhu, J.W.; Wang, M.C. Mechanical properties and microstructure of a graphene oxide–cement composite. *Cem. Concr. Compos.* **2015**, *58*, 140–147. [CrossRef]
21. Wang, Y.W.; Cao, A.; Jiang, Y.; Zhang, X.; Liu, J.H.; Liu, Y.; Wang, H. Superior antibacterial activity of zinc oxide/graphene oxide composites originating from high zinc concentration localized around bacteria. *ACS Appl. Mater. Interf.* **2014**, *6*, 2791–2798. [CrossRef] [PubMed]
22. Lucas, S.S.; Ferreira, V.M.; De Aguiar, J.B. Incorporation of titanium dioxide nanoparticles in mortars—Influence of microstructure in the hardened state properties and photocatalytic activity. *Cem. Concr. Res.* **2013**, *43*, 112–120. [CrossRef]
23. Gunschera, J.; Andersen, J.R.; Schulz, N.; Salthammer, T. Surface-catalysed reactions on pollutant-removing building products for indoor use. *Chemosphere* **2009**, *75*, 476–482. [CrossRef]

24. Hunger, M.; Hüsken, G.; Brouwers, J. Photocatalysis applied to concrete products. *ZKG Int.* **2008**, *61*, 76–84.
25. Fujishima, A.; Zhang, X.; Tryk, D.A. TiO2 photocatalysis and related surface phenomena. *Surf. Sci. Rep.* **2008**, *63*, 515–582. [CrossRef]
26. Noeiaghaei, T.; Dhami, N.; Mukherjee, A. Nanoparticles surface treatment on cemented materials for inhibition of bacterial growth. *Constr. Build. Mater.* **2017**, *150*, 880–891. [CrossRef]
27. Ibrahim, N.M.; Malek, R.A.; Rahim, N.L.; Rahim, M.A.; Amat, R.C.; Mohammed, S.A.; Badri, N.A. Exploring the Properties of Mortar Containing Incineration Fly Ash. *IOP Conf. Ser. Earth Environ. Sci.* **2021**, *920*, 12041. [CrossRef]
28. Gao, Y.; Jing, H.; Fu, G.; Zhao, Z.; Shi, X. Studies on combined effects of graphene oxide-fly ash hybrid on the workability, mechanical performance and pore structures of cementitious grouting under high W/C ratio. *Constr. Build. Mater.* **2021**, *281*, 122578. [CrossRef]
29. Kırgız, M.S. Advancements in properties of cement containing pulverised fly ash and nanomaterials by blending and ultrasonication method (Review-Part II). *Nano Hybrids Compos.* **2019**, *24*, 37–44. [CrossRef]
30. Popa, D.; Prodan, D.; Varvara, S.; Popa, M.; Cuc, S.; Sarosi, C.; Moldovan, M.; Ivan, R.; Ene, R. Properties evolution of some hydraulic mortars incorporating graphene oxides. *Buildings* **2022**, *12*, 864. [CrossRef]
31. Prodan, D.; Moldovan, M.; Furtos, G.; Saroși, C.; Filip, M.; Perhaița, I.; Carpa, R.; Popa, M.; Cuc, S.; Varvara, S.; et al. Synthesis and characterization of some graphene oxide powders used as additives in hydraulic mortars. *Appl. Sci.* **2021**, *11*, 11330. [CrossRef]
32. Pozo-Antonio, J.S. Evolution of mechanical properties and drying shrinkage in lime-based and lime cement-based mortars with pure limestone aggregate. *Constr. Build. Mater.* **2015**, *77*, 472–478. [CrossRef]
33. Vuppaladadium, S.S.R.; Agarwal, T.; Kulanthaivel, S.; Mohanty, B.; Barik, C.S.; Maiti, T.K.; Banerjee, I. Silanization improves biocompatibility of graphene oxide. *Mater. Sci. Eng. C* **2020**, *110*, 110647. [CrossRef]
34. *CEN, EN 1015-18:2002*; Methods of Test for Mortar for Masonry. Part 18: Determination of Water Absorption Coefficient Due to Capillary Action of Hardened Mortar. European Committee for Standardization: Brussels, Belgium, 2002.
35. *CEN, EN 15801:2009*; Conservation of Cultural Property. Test Methods: Determination of Water Absorption by Capillarity. European Committee for Standardization: Brussels, Belgium, 2009.
36. Gulotta, D.; Goidanich, S.; Tedeschi, C.; Nijland, T.G.; Toniolo, L. Commercial NHL-containing mortars for the preservation of historical architecture. Part 1: Compositional and mechanical characterisation. *Constr. Build. Mater.* **2013**, *38*, 31–42. [CrossRef]
37. Mohammed, A.; Sanjayan, J.G.; Duan, W.H.; Nazari, A. Incorporating graphene oxide in cement composites: A study of transport properties. *Constr. Build. Mater.* **2015**, *84*, 341–347. [CrossRef]
38. Kurantowicz, N.; Sawosz, E.; Jaworski, S.; Kutwin, M.; Strojny, B.; Wierzbicki, M. Interaction of graphene family materials with Listeria monocytogenes and Salmonella enterica. *Nano. Res. Lett.* **2015**, *10*, 23. [CrossRef]
39. Zou, F.; Zhou, H.; Jeong, D.Y.; Kwon, J.; Eom, S.U.; Park, T.J. Wrinkled surface-mediated antibacterial activity of graphene oxide nanosheets. *ACS Appl. Mater. Interf.* **2017**, *9*, 1343–1351. [CrossRef] [PubMed]
40. Pang, L.; Dai, C.; Bi, L.; Guo, Z.; Fan, J. Biosafety and antibacterial ability of graphene and graphene oxide in vitro and in vivo. *Nano. Res. Lett.* **2017**, *12*, 564. [CrossRef] [PubMed]
41. Zhang, L.; Jiang, Y.; Ding, Y.; Povey, M.; York, D. Investigation into the antibacterial behaviour of suspensions of ZnO nanoparticles (ZnO nanofluids). *J. Nanoparti. Resear.* **2007**, *9*, 479. [CrossRef]
42. Jones, N.; Ray, B.; Ranjit, K.T.; Manna, A.C. Antibacterial activity of ZnO nanoparticle suspensions on a broad spectrum of microorganisms. *FEMS Microbiol. Lett.* **2008**, *279*, 71. [CrossRef]
43. Jiang, W.; Mashayekhi, H.; Xing, B. Bacterial toxicity comparison between nano- and micro-scaled oxide particles. *Environ. Pollut.* **2009**, *157*, 1619. [CrossRef] [PubMed]
44. Subhan, M.A.; Awal, M.R.; Ahmed, T.; Younus, M. Photocatalytic and antibacterial activities of Ag/ZnO nano-composities fabricated by co-precipitation method. *Acta Metall. Sin. Engl. Lett.* **2014**, *27*, 223. [CrossRef]
45. Emami-Karvani, Z.; Chehrazi, P. Antibacterial activity of ZnO nanoparticle on grampositive and gram-negative bacteria. *Afr. J. Microbiol. Resear.* **2011**, *5*, 1368. [CrossRef]
46. Kathirvelu, S.; D'Souza, L.; Dhurai, B. A study on functional finishing of cotton fabrics using nanoparticles of zinc oxide. *Mater. Sci.* **2009**, *15*, 75.

Disclaimer/Publisher's Note: The statements, opinions and data contained in all publications are solely those of the individual author(s) and contributor(s) and not of MDPI and/or the editor(s). MDPI and/or the editor(s) disclaim responsibility for any injury to people or property resulting from any ideas, methods, instructions or products referred to in the content.